



Article

Systematic Analysis of Transcriptomic Profile of Chondrocytes in Osteoarthritic Knee Using Next-Generation Sequencing and Bioinformatics

Yi-Jen Chen ^{1,2}, Wei-An Chang ^{1,3}, Ling-Yu Wu ¹, Ya-Ling Hsu ⁴, Chia-Hsin Chen ^{2,5,6,*} and Po-Lin Kuo ^{1,7,*} 

¹ Graduate Institute of Clinical Medicine, College of Medicine, Kaohsiung Medical University, Kaohsiung 807, Taiwan; chernkmu@gmail.com (Y.-J.C.); 960215kmuh@gmail.com (W.-A.C.); esther906@gmail.com (L.-Y.W.)

² Department of Physical Medicine and Rehabilitation, Kaohsiung Medical University Hospital, Kaohsiung 807, Taiwan

³ Division of Pulmonary and Critical Care Medicine, Kaohsiung Medical University Hospital, Kaohsiung 807, Taiwan

⁴ Graduate Institute of Medicine, College of Medicine, Kaohsiung Medical University, Kaohsiung 807, Taiwan; hsuy1326@gmail.com

⁵ Department of Physical Medicine and Rehabilitation, School of Medicine, College of Medicine, Kaohsiung Medical University, Kaohsiung 807, Taiwan

⁶ Orthopaedic Research Center, Kaohsiung Medical University, Kaohsiung 807, Taiwan

⁷ Institute of Medical Science and Technology, National Sun Yat-Sen University, Kaohsiung 804, Taiwan

* Correspondence: chchen@kmu.edu.tw (C.-H.C.); kuopolin@seed.net.tw (P.-L.K.);

Tel.: +886-7-312-1101 (ext. 5962) (C.-H.C.); +886-7-312-1101 (ext. 2512-33) (P.-L.K.)

Received: 12 October 2018; Accepted: 7 December 2018; Published: 10 December 2018



Abstract: The phenotypic change of chondrocytes and the interplay between cartilage and subchondral bone in osteoarthritis (OA) has received much attention. Structural changes with nerve ingrowth and vascular penetration within OA cartilage may contribute to arthritic joint pain. The aim of this study was to identify differentially expressed genes and potential miRNA regulations in OA knee chondrocytes through next-generation sequencing and bioinformatics analysis. Results suggested the involvement of SMAD family member 3 (*SMAD3*) and Wnt family member 5A (*WNT5A*) in the growth of blood vessels and cell aggregation, representing features of cartilage damage in OA. Additionally, 26 dysregulated genes with potential miRNA–mRNA interactions were identified in OA knee chondrocytes. Myristoylated alanine rich protein kinase C substrate (*MARCKS*), ephregulin (*EPREGLIN*), leucine rich repeat containing 15 (*LRRCL15*), and phosphodiesterase 3A (*PDE3A*) expression patterns were similar among related OA cartilage, subchondral bone and synovial tissue arrays in Gene Expression Omnibus database. The Ingenuity Pathway Analysis identified *MARCKS* to be associated with the outgrowth of neurite, and novel miRNA regulations were proposed to play critical roles in the pathogenesis of the altered OA knee joint microenvironment. The current findings suggest new perspectives in studying novel genes potentially contributing to arthritic joint pain in knee OA, which may assist in finding new targets for OA treatment.

Keywords: knee osteoarthritis; cartilage damage; chondrocytes; joint pain; next-generation sequencing; bioinformatics; microRNA; messenger RNA

1. Introduction

Osteoarthritis (OA) is one of the common musculoskeletal disorders with increased incidence in the elderly [1]. The diagnosis of OA is based on clinical symptoms and radiographic findings,

such as narrowed joint space and irregular cortical surface with the presence of osteophytes; the clinical symptoms of OA include pain, swelling and joint deformity that impede normal walking [2,3]. The cardinal pathological change in the OA joint is the destruction of articular cartilage. During degeneration and OA changes, chondrocytes shift towards a hypertrophic phenotype, and proliferation and hypertrophic differentiation of chondrocytes occur, with the characteristics of decreased synthesis of the extracellular matrix (ECM) and increased production of proteolytic enzymes such as metalloproteinases (MMPs), resulting in remodeling and mineralization of ECM [4,5]. Hypertrophic chondrocytes also promote angiogenesis in OA [6].

The biological functions of chondrocytes and histopathological changes of articular cartilage in OA have been extensively studied [5,7]. While cartilage breakdown is the major consequence of OA, there is a growing consensus that OA is considered a disease of the entire joint, affecting all tissues in the joint, including cartilage, subchondral bone, meniscus, ligament, and synovium, and is not merely a process of wear and tear [8]. Of note, the interplay between cartilage and subchondral bone, mainly mediated by chondrocytes and osteoblasts within the two compartments, has received much attention and potentially contributes to the pathogenesis of OA [4]. The abnormal remodeling and increased vascularization observed in the OA joint facilitate molecular transport and cellular interaction between cartilage and bone [9].

MicroRNAs (miRNAs) are small non-coding single-stranded RNAs that regulate gene expression through binding to the 3' untranslated region (UTR) of target mRNAs [10]. The functions of miRNAs have been shown to play critical roles in the pathogenesis of OA, regulating the gene expressions of several proteolytic enzymes and influencing various growth factor signaling pathways [10–12]. The advanced technology of high-throughput next-generation sequencing (NGS) has made available a rapid gain of a large volume of genomic data [13], and the use of bioinformatics approaches to analyze these large datasets gives better understanding and more rapid analysis of associations and biological functions of selected lists of genes and/or miRNAs [14–16]. In the current study, different bioinformatics databases and tools were used to recognize biological functions and potential miRNA–mRNA interactions involved in OA chondrocytes, including Ingenuity Pathway Analysis (IPA) [17], Database for Annotation, Visualization and Integrated Discovery (DAVID) [18], Gene Expression Omnibus (GEO) [19], and miRmap [20,21]. Using the NGS and extensive bioinformatics analysis, we aim to identify novel miRNAs and potential miRNA regulations of target genes differentially expressed in OA chondrocytes. We expect the findings will provide new perspectives in the pathogenesis and potential therapeutic targets for patients with OA.

2. Materials and Methods

2.1. Cell Culture

Chondrocytes of normal adult and osteoarthritic knee cartilage were purchased from Cell Applications, Inc. (San Diego, CA, USA), which were cryopreserved at the first passage. Chondrocytes were cultured in Chondrocyte Growth Medium (Cell Applications, Inc. San Diego, CA, USA) and placed in a 37 °C, 5% CO₂ humidified incubator until confluence, at 7 days after seeding. The normal and OA knee chondrocytes were then harvested for total RNA extraction and further expression profiling of mRNA and small RNA.

2.2. RNA Sequencing

Total RNAs of normal and OA knee chondrocytes were extracted using Trizol Reagent (Invitrogen, Carlsbad, CA, USA) following the manufacturer's instructions and the quality of extracted RNAs were analyzed for OD₂₆₀ detection by ND-1000 spectrophotometer (Nanodrop Technology, Wilmington, DE, USA) before sequencing. The quality of extracted RNAs were validated by RNA integrity number (RIN) with Agilent Bioanalyzer (Agilent Technology, Santa Clara, CA, USA), with RIN of 9.8 for normal knee chondrocytes and 9.9 for OA knee chondrocytes. The sequencing analysis for RNA and small RNA

were carried out by Welgene Biotechnology Company (Welgene, Taipei, Taiwan). For RNA sequencing, the library preparation and sequencing procedures were carried out following the manufacture's protocol from Illumina. A read length of 75 nucleotides single-end sequencing on Solexa platform was performed for library construction, the sequence was determined using sequencing-by-synthesis technology, and raw sequences obtained from Illumina Pipeline software bcl2fastq v2.0 generated 30 million reads per sample. The raw sequences were filtered and trimmed for qualified reads, and TopHat/Cufflinks method was used for gene expression estimation. The expression level was normalized by calculating fragments per kilobase of transcript per million mapped reads (FPKM). The reference genome and gene annotations were obtained from Ensembl database. For small RNA sequencing, library construction was prepared using Illumina sample preparation kit, following the TruSeq Small RNA Sample Preparation Guide. The 3' and 5' adaptors were ligated to total RNA, reverse transcribed, and PCR amplified. The cDNA constructs were fractionated and purified for bands containing 18–40 nucleotide RNA fragments. The prepared libraries were sequenced with a read length of 75 nucleotides single-end and processed with Illumina instrument and software. The raw sequences were filtered and trimmed for qualified reads, analyzed in miRDeep2 to clip 3' adaptor sequence, and aligned to the human genome from University of California, Santa Cruz (UCSC). All reads were normalized by Reads Per Million (RPM) [22]. The miRDeep2 was used to estimate expression levels of known and novel miRNAs. The sequencing quality for both RNA and small RNA was determined by FastQC, a quality control tool for high-throughput sequence data, reporting per-base sequence quality and per-sequence quality scores. The criteria of differentially expressed mRNAs and miRNAs were set at fold change >2.0, FPKM >0.3 for mRNA and RPM >10 for miRNA. The threshold of FPKM >0.3 for mRNA was selected, since lower confidence in measured expression levels below 0.3 was reported [23]. The threshold of RPM >10 for miRNA was selected to identify functional miRNAs as previously reported [24].

2.3. Ingenuity Pathway Analysis (IPA)

The Ingenuity Pathway Analysis (IPA) software (Ingenuity systems, Redwood City, CA, USA) provides bioinformatics analysis of gene arrays; RNA and small RNA sequencing, proteomics and other biological experiments; categorizes molecules into different biological networks; and identifies related canonical pathways, upstream regulators, diseases and functions involved in a subset of molecules. The IPA core analysis provides predicted canonical pathways based on the literature and *de novo* network discovery based on expression changes of uploaded experimental results [17]. Additionally, construction of causal networks based on gene interactions curated from the literature is also available, which provides mechanistic hypotheses based on expression changes of the uploaded dataset. The statistical significance of the constructed regulatory networks was determined by Fisher's exact test *p*-value (enrichment score) that measured the overlap of observed and predicted gene sets, and Z score that measured the match of observed and predicted regulatory patterns with directional effect [25]. In the current study, differentially expressed genes with fold changes in expression between normal and OA knee chondrocytes were uploaded into IPA for core analysis to obtain pathway and network results. For "create expression analysis" setting, we took into consideration all direct and indirect relationships identified in all data sources with experimentally observed or moderate to highly predicted confidence, without specifying tissue types or species.

2.4. Database for Annotation, Visualization and Integrated Discovery (DAVID) Bioinformatics Resources

The DAVID bioinformatics resources is an open-source bioinformatics database that provides an integrated data-mining environment and categorizes a list of genes into different biological functions using different tools such as functional annotation and gene functional classification. Users are able to have an overall concept of the biological themes that are enriched in the list of genes [18]. Differentially expressed genes of interest were input into DAVID database for functional annotation

analysis, and the Expression Analysis Systematic Explorer (EASE) score was set at a default cutoff value of 0.1, representing the modified Fisher's exact p -value in the DAVID database.

2.5. Gene Expression Omnibus (GEO) Database

The GEO database provides high-throughput genomic data sets, and researchers can have access to the analysis of genes of interest and their expression values through web-based tools such as GEO2R, and perform further between-group comparisons [19]. The relevant datasets related to joint tissues of OA patients (GSE114007 for cartilages, GSE51588 for subchondral bones, GSE55235 and GSE55457 for synovial tissues) were used in this study to examine whether the expression patterns of genes of interest were in line with that observed in our expression profile of OA knee chondrocytes. Detailed information of the selected datasets was provided in .

2.6. miRmap Database

MiRmap is an open-source software library developed by Vejnar et al. that is available online. The library provides miRNA target prediction by ranking the repression strength of potential targets. The repression strength is predicted by a comprehensive approach, combining thermodynamic, evolutionary, probabilistic and sequence-based features, and is given a miRmap score for each potential target. The higher score indicates higher repression strength. In our current study, the 46 differentially expressed miRNAs were sequentially inputted into the library to obtain potential target genes. Those potential targets with miRmap scores higher than 99.0 were selected for further analysis [20,21].

2.7. Statistical Analysis

To determine differentially expressed mRNAs between normal and OA knee chondrocytes, statistical analysis was performed using Cuffdiff (Cufflinks version 2.2.1), with p -value calculation for non-grouped samples using blind mode, in which all samples were treated as replicates of a single global condition and used to build one model for a statistic test [26]. Based on the selection of competitive null hypothesis and the use of over-representation analysis as the pathway analysis method for our pathway annotation analysis [16,27], we firstly selected from our high-throughput differential expression data those mRNAs with expression values of FPKM >0.3, a fold-change >2.0 and a p -value <0.05 between normal and OA knee chondrocytes. Further, multiple testing correction for p -value adjustments using Bonferroni adjustment method, Hochberg's method and false discovery rate (FDR) controlling method [28,29] was performed using Statistical Analysis System (SAS) PROC MULTTEST (SAS version 9.4, SAS Institute, Cary, NC, USA) for the pre-selected differential expression gene list. An adjusted p -value of <0.05 indicated statistical significance. All pre-selected differential expression genes remained statistically significant after Hochberg's method and FDR controlling method corrections. In addition, expression values of target genes in OA and non-OA patients identified from selected GEO arrays were analyzed for between-group differences, using IBM SPSS Statistics for Windows, version 19 (IBM Corp., Armonk, NY, USA). For the relatively small numbers of cases in each group, the non-parametric method with the Mann-Whitney U test was used for between-group comparison. A p -value < 0.05 was considered as a statistically significant difference.

3. Results

3.1. The Sequencing Quality and Mapped Reads for RNA and Small RNA Sequencing of Chondrocytes

The results of sequencing quality of RNA sequencing for normal and OA knee chondrocytes, using FastQC, are shown in Figure S1, reporting high quality scores in per-base sequence quality and per-sequence quality scores. Similarly, the quality scores of small RNA sequencing for normal and OA knee chondrocytes indicated good sequencing quality (Figure S2). The mapped reads for both RNA and small RNA sequencing are listed in Table S2. The raw sequencing data were uploaded to

the GEO repository with the GEO accession number of GSE110606. The data will be held private before publication.

3.2. The Differentially Expressed Genes in Osteoarthritic Knee Chondrocytes were Associated with Osteoarthritis Pathway, Cell Adhesion and Extracellular Matrix Organization

The expression values of normal and OA knee chondrocytes were obtained from the NGS results of RNA-sequencing and were further analyzed. Screening for gene expressions with FPKM >0.3, the difference in FPKM performance between normal and OA knee chondrocytes was displayed as a density plot, as indicated in Figure 1A. A total of 495 differentially expressed protein-coding genes with >2.0-fold-change and >0.3 FPKM were identified, where 263 genes were up-regulated and 232 genes were down-regulated in OA knee chondrocytes, compared to normal chondrocytes. The detailed information of the 495 differentially expressed genes is provided in Table S3. To determine the biological functions and pathways possibly involved in these differentially expressed genes in chondrocytes, we use the IPA software and the functional annotation tool in the DAVID database for further analysis. The results of IPA analysis identified the osteoarthritis pathway as the most highly enriched canonical pathway among these dysregulated genes, with 23 differentially expressed genes involved in this pathway ($p = 4.72 \times 10^{-10}$, Z score = 1.342), and tumor necrosis factor (*TNF*) as the most highly predicted upstream regulator ($p = 2.20 \times 10^{-22}$, Z score = -0.159). The top five canonical pathways and potential upstream regulators are listed in Table 1.

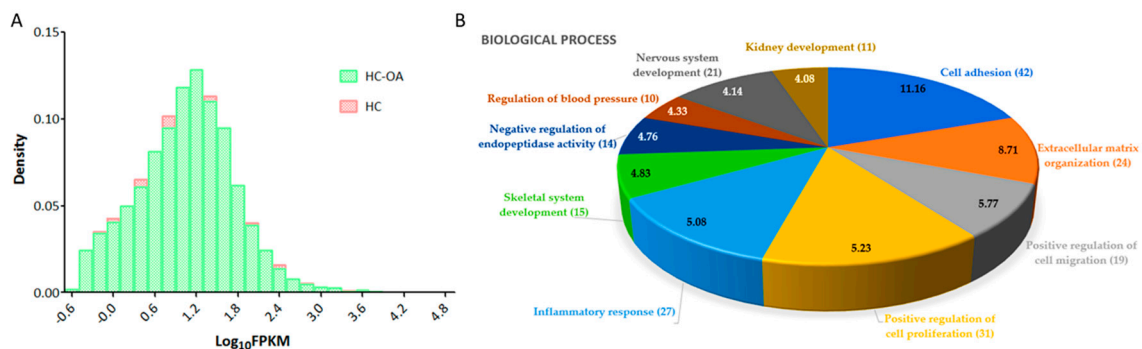


Figure 1. Differential expression analysis of genes in osteoarthritic (OA) knee chondrocytes. (A) For gene expressions with fragments per kilobase of transcript per million (FPKM) >0.3, the difference in FPKM performance between normal (HC) and OA (HC-OA) knee chondrocytes is shown in a density plot. The x-axis represents logarithm to the base 10 of FPKM, and the y-axis indicates read density. (B) The 495 differentially expressed protein-coding genes in OA knee chondrocytes were input into the DAVID database to determine related biological functions, and these dysregulated genes were related to cell adhesion (42 genes), extracellular matrix organization (24 genes), positive regulation of cell migration (19 genes), positive regulation of cell proliferation (31 genes), inflammatory response (27 genes), skeletal system development (15 genes), negative regulation of endopeptidase activity (14 genes), regulation of blood pressure (10 genes), nervous system development (21 genes), and kidney development (11 genes). The selected criteria for functional annotation analysis were Expression Analysis Systematic Explorer (EASE) score = 0.1 and fold enrichment >1.3. The $-\log(p \text{ value})$ of each biological term is indicated within the pie chart.

Table 1. Top canonical pathways and upstream regulators involved in differentially expressed genes of osteoarthritic (OA) knee chondrocytes.

Category	No. of Genes	p-Value
Top canonical pathways		
Osteoarthritis Pathway	23	4.72×10^{-10}
Hepatic Fibrosis/Hepatic Stellate Cell Activation	20	8.99×10^{-9}
Axonal Guidance Signaling	31	4.32×10^{-8}
Atherosclerosis Signaling	15	1.77×10^{-7}
GP6 Signaling Pathway	13	1.06×10^{-5}
Top predicted upstream regulators		
<i>TNF</i>		2.20×10^{-22}
<i>TGFB1</i>		1.01×10^{-21}
Dexamethasone		1.57×10^{-16}
<i>IFNG</i>		6.75×10^{-16}
<i>CTNNB1</i>		1.50×10^{-15}

CTNNB1, catenin beta 1; *IFNG*, interferon gamma; *TGFB1*, transforming growth factor beta 1; *TNF*, tumor necrosis factor.

Through the functional annotation analysis in the DAVID database, the top 10 biological processes involved in these differentially expressed genes were identified to be related to cell adhesion (42 genes, $p = 6.87 \times 10^{-12}$, false discovery rate (FDR) = 1.22×10^{-8}), extracellular matrix organization (24 genes, $p = 1.94 \times 10^{-9}$, FDR = 3.43×10^{-6}), positive regulation of cell migration (19 genes, $p = 1.71 \times 10^{-6}$, FDR = 0.003), positive regulation of cell proliferation (31 genes, $p = 5.95 \times 10^{-6}$, FDR = 0.011), inflammatory response (27 genes, $p = 8.25 \times 10^{-6}$, FDR = 0.015), skeletal system development (15 genes, $p = 1.47 \times 10^{-5}$, FDR = 0.026), negative regulation of endopeptidase activity (14 genes, $p = 1.73 \times 10^{-5}$, FDR = 0.031), regulation of blood pressure (10 genes, $p = 4.67 \times 10^{-5}$, FDR = 0.083), nervous system development (21 genes, $p = 7.31 \times 10^{-5}$, FDR = 0.130), and kidney development (11 genes, $p = 8.24 \times 10^{-5}$, FDR = 0.146), as shown in Figure 1B. The functional annotation clustering analysis of the 495 differentially expressed genes indicated the enrichment score of 2.47 for a group of genes related to biological functions of cartilage and bone. In addition, other significant biological functions ($p < 0.05$, fold enrichment >1.3) related to cellular, tissue and structural changes in OA joint, including regulation of cartilage development, chondrocyte differentiation and bone mineralization, endochondral ossification, and the corresponding differentially expressed genes are listed in Table 2. A total of nine up-regulated genes and six down-regulated genes in the OA knee chondrocytes were identified.

Table 2. Selected biological functions related to cellular, tissue and structural changes in osteoarthritis.

Biological Process	Count	p-Value	Up-Regulated Genes	Down-Regulated Genes	Fold Enrichment
Positive regulation of bone mineralization	7	2.66×10^{-4}	<i>BMP4, GPM6B, P2RX7, SMAD3, TMEM119</i>	<i>BMP2, BMP6</i>	7.62
Positive regulation of chondrocyte differentiation	5	1.32×10^{-3}	<i>ACVRL1, GDF6, SMAD3</i>	<i>BMP6, SOX9</i>	10.02
Positive regulation of cartilage development	4	7.76×10^{-3}	<i>BMP4, WNT5A</i>	<i>BMP2, SOX9</i>	9.52
Chondrocyte differentiation	5	1.86×10^{-2}	<i>BMP4</i>	<i>BMP2, COL11A2, CYTL1, FGFR3</i>	4.88
Endochondral ossification	4	2.97×10^{-2}	<i>ALPL, BMP4</i>	<i>BMP6, FGFR3</i>	5.86

3.3. Identification of Dysregulated Genes Related to Joint Structural Damage in OA

To investigate the expression patterns of genes related to biological processes of cellular, tissue and structural changes in OA joint in clinical specimens, we searched in the GEO database for OA-related datasets. One RNA sequencing dataset consisting of 18 normal knee cartilages and 20 OA knee cartilages was found (GSE114007). One array comparing the expression profiles of subchondral bones at medial and lateral tibial plateaus of both normal and OA knee joints was also found (GSE51588). Considering the close contact of cartilage and subchondral bones and possible crosstalk between these joint tissues in the OA joint microenvironment, we simultaneously investigated the expression patterns of these genes in the subchondral bone dataset. The results showed that the expression patterns of *ACVRL1*, *ALPL*, *GDF6*, *TMEM119*, *WNT5A*, *CYTL1*, and *SOX9* in OA knee cartilages were consistent with our expression profile of OA chondrocytes (Figure 2A,B), while the expression patterns of *ACVRL1*, *ALPL*, *BMP4*, *GDF6*, *SMAD3*, *TMEM119*, and *WNT5A* in subchondral bones of OA knees were consistent with our data (Figure 3A,B).

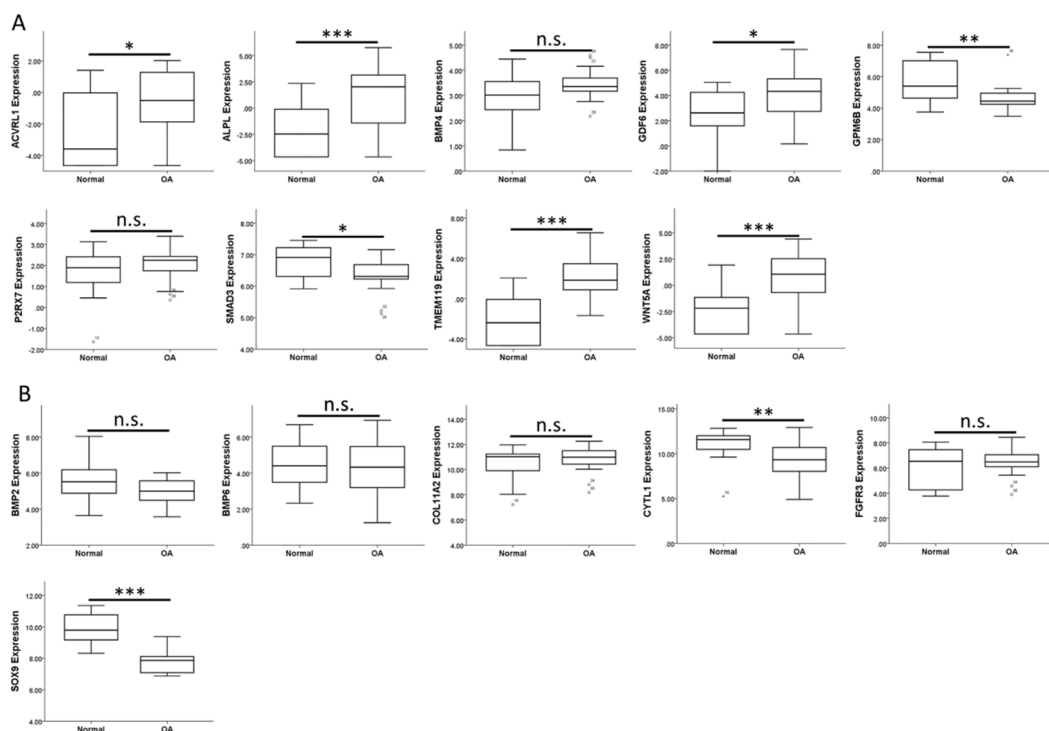


Figure 2. Expression patterns of genes related to the biological processes of OA in the GEO dataset of OA knee cartilages. The expression patterns of (A) 9 up-regulated genes and (B) 6 down-regulated genes related to biological processes of cellular, tissue and structural changes in OA were analyzed in a GEO dataset of normal and OA knee cartilages (GSE114007). *ACVRL1*, *ALPL*, *GDF6*, *TMEM119*, and *WNT5A* were significantly up-regulated, whereas *CYTL1* and *SOX9* were significantly down-regulated in OA knee cartilages. The expression patterns of *GPM6B* and *SMAD3* (down-regulated) in OA knee cartilage were different from that identified in our expression profile of OA knee chondrocytes (up-regulated). * indicated $p < 0.05$, ** indicated $p < 0.01$, *** indicated $p < 0.001$, and n.s. indicated no statistical significance between normal and OA groups.

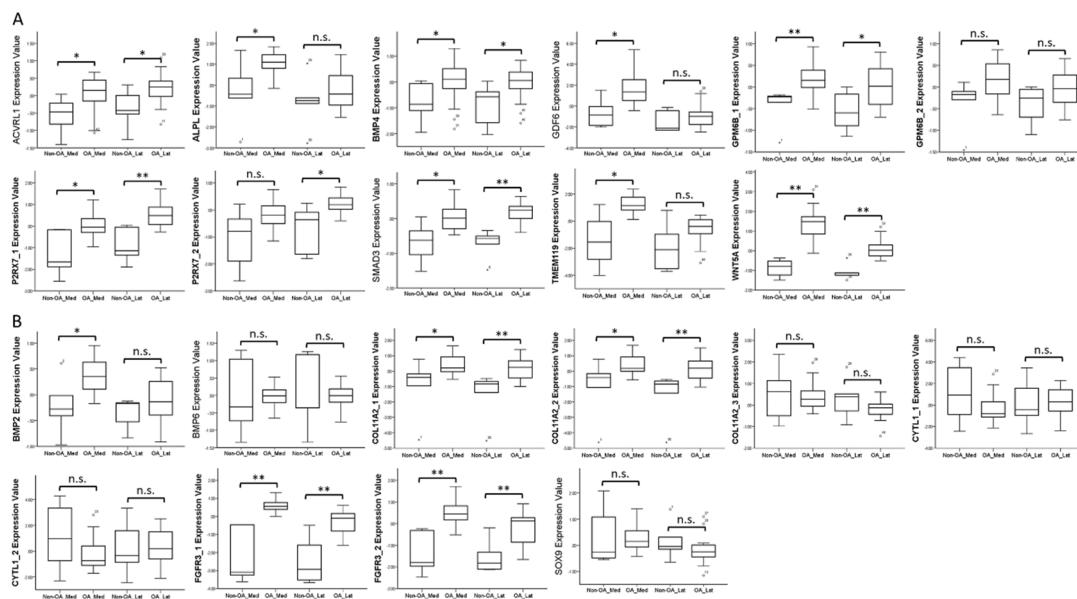


Figure 3. Expression patterns of genes related to biological processes of OA in GEO array of OA knee subchondral bone. The expression patterns of (A) nine up-regulated genes and (B) six down-regulated genes related to the biological processes of cellular, tissue and structural changes in OA were analyzed in a GEO array of normal and OA knee subchondral bone (GSE51588). *ACVRL1*, *BMP4*, *SMAD3*, and *WNT5A* were significantly up-regulated in both medial and lateral plateaus, whereas *ALPL*, *GDF6*, and *TMEM119* were significantly up-regulated only in the medial plateau of OA knees. The expression patterns of *BMP2*, *COL11A2*, and *FGFR3* (up-regulated) in subchondral bones of OA knees were different from that identified in our expression profile of OA knee chondrocytes (down-regulated). * indicated $p < 0.05$, ** indicated $p < 0.01$, and n.s. indicated no statistical significance between non-OA and OA groups. For those genes with more than one probe within the array, the expression patterns were considered consistent only if there were at least two probes with significant dysregulation in the same direction. (Probe ID reference: *ACVRL1*, A_24_P945113; *ALPL*, A_24_P353619; *BMP4*, A_23_P54144; *GDF6*, A_32_P140489; *GPM6B_1*, A_33_P3218649; *GPM6B_2*, A_23_P378416; *P2RX7_1*, A_24_P319113; *P2RX7_2*, A_33_P3263867; *SMAD3*, A_23_P48936; *TMEM119*, A_33_P3395605; *WNT5A*, A_33_P3341499; *BMP2*, A_33_P3237150; *BMP6*, A_23_P19624; *COL11A2_1*, A_33_P3216442; *COL11A2_2*, A_23_P42322; *COL11A2_3*, A_33_P3216448; *CYTL1_1*, A_33_P3252695; *CYTL1_2*, A_23_P10647; *FGFR3_1*, A_23_P500501; *FGFR3_2*, A_23_P212830; and *SOX9*, A_23_P26847).

3.4. *SMAD3* and *WNT5A* were Involved in Growth of Blood Vessel and Cell Aggregation

Diseases and functions related to cellular, tissue and structural changes of cartilage in OA analyzed in the IPA software were selected, including osteoarthritis ($p = 5.53 \times 10^{-11}$, Z score = 0.762), abnormality of cartilage tissue ($p = 5.06 \times 10^{-7}$, Z score = 1.000), differentiation of chondrocytes ($p = 6.60 \times 10^{-8}$, Z score = -0.265), growth of blood vessel ($p = 4.29 \times 10^{-7}$, Z score = 0), and aggregation of cells ($p = 1.15 \times 10^{-9}$, Z score = 2.262); the merged network of these diseases and functions is shown in Figure 4. Among the seven significantly dysregulated genes identified in the previous section, we found that *SMAD3* was centered to the merged network, and interconnected with molecules of other networks, including those in the growth of blood vessel, a feature of cartilage damage in OA [9]. In addition, *WNT5A* was involved in the aggregation of cells related to the formation of chondrocyte clusters in OA [7,9,30].

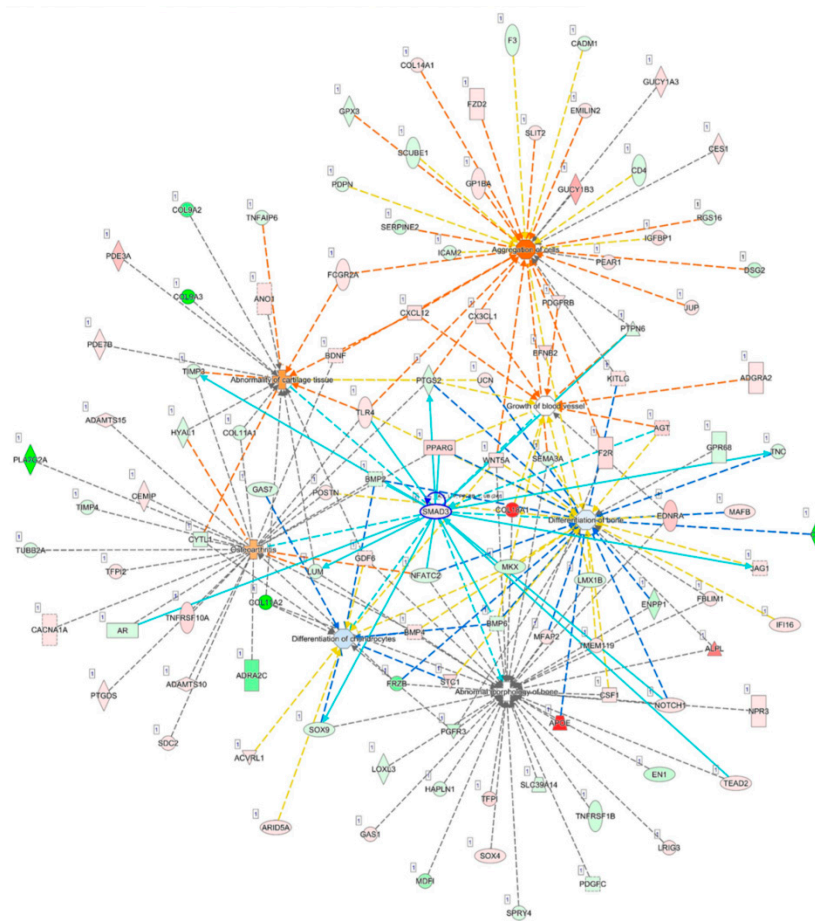


Figure 4. Analysis of interconnections and the merged network of OA-related diseases and functions. The 495 differentially expressed genes identified in OA knee chondrocytes were analyzed in the Ingenuity Pathway Analysis (IPA) software, and diseases and functions related to cellular, tissue and structural changes of cartilage in OA, including osteoarthritis, abnormality of cartilage tissue, differentiation of chondrocytes, growth of blood vessel, and aggregation of cells, were selected to identify target genes involved. *SMAD3* was centered to the merged network and interconnected with the molecules of other networks, as indicated in light blue lines, including those in the growth of the blood vessel. *WNT5A* was involved in aggregation of cells, which was possibly associated with the formation of chondrocyte clusters in OA.

3.5. Identification of Differentially Expressed miRNAs and Potential miRNA–mRNA Interactions between Normal and OA Knee Chondrocytes

To determine the potential miRNA–mRNA interactions between normal and OA knee chondrocytes, we also performed small RNA sequencing by NGS, and identified 46 differentially expressed miRNAs (>2.0-fold change and >10 RPM of either origin of chondrocytes), including nine up-regulated and 37 down-regulated miRNAs in OA knee chondrocytes compared to normal chondrocytes. The detailed information of the 46 differentially expressed miRNAs is provided in Table S4. The heat map of the 46 differentially expressed miRNAs with z-score values is shown in Figure 5A. The putative targets of the 46 miRNAs were predicted using miRmap database and selected targets with miRmap score >99.0. The analytical results yielded 274 putative targets of nine up-regulated miRNAs and 1041 putative targets of 37 down-regulated miRNAs. The 274 targets of up-regulated miRNAs and 1041 targets of down-regulated miRNAs were then matched to our 232 down-regulated genes and 263 up-regulated genes obtained from high-throughput RNA sequencing, respectively. Using the Venn diagram analysis available on the website [31], four down-regulated genes and 22

up-regulated genes with potential miRNA-mRNA interactions in OA chondrocytes were identified, as depicted in Figure 5B.

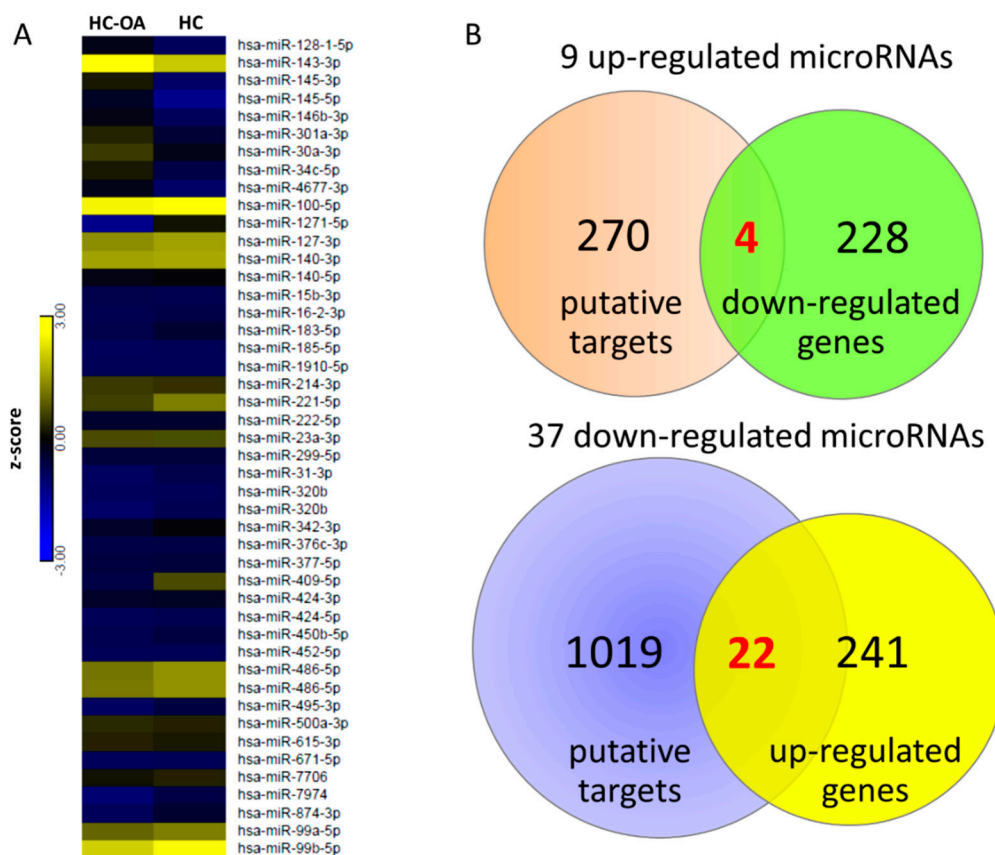


Figure 5. Identification of dysregulated miRNAs and potential miRNA–mRNA interactions in OA knee chondrocytes. (A) The 46 differentially expressed miRNAs of OA chondrocytes (>2.0-fold change and reads per million (RPM) > 10) were identified from the next-generation sequencing (NGS) result, and the heat map with z-score values is shown. (B) The miRmap database analysis identified 274 putative targets of nine up-regulated miRNAs and 1041 putative targets of 37 down-regulated miRNAs (selection threshold set at miRmap score ≥ 99.0). In addition, 232 down-regulated genes and 263 up-regulated genes (>2.0-fold change and fragments per kilobase of transcript per million (FPKM) > 0.3) in OA chondrocytes were identified from the NGS results. The putative targets of up-regulated (down-regulated) miRNAs were matched to our down-regulated (up-regulated) protein-coding genes using the Venn diagram analysis, which yielded four down-regulated genes and 22 up-regulated genes with potential miRNA–mRNA interactions in OA knee chondrocytes.

3.6. Analysis of Candidate Genes with Potential miRNA-mRNA Interactions in Gene Expression Omnibus (GEO) Database and Identification of Potential Molecular Signatures in OA Knee Joint Microenvironment

The 26 candidate genes with potential miRNA–mRNA interactions are listed in Table 3. We searched in the GEO database for OA-related datasets to further determine the expression patterns of these candidate genes in clinical specimen. Since OA is considered a disease involving all joint tissues, we took datasets of cartilage, subchondral bone and synovium into consideration while searching for related datasets. There were two representative arrays analyzing synovial tissues of non-arthritis and OA patients (GSE55235 and GSE55457). Along with the datasets of cartilages and subchondral bones from knee OA patients used in the previous section (GSE114007 and GSE51588), the expression patterns of the 26 candidate genes were sequentially analyzed in these four representative datasets to determine genes potentially dysregulated in the OA microenvironment, and are summarized in Table 4. The up-regulated *MARCKS* was found up-regulated in OA knee cartilages, subchondral

bones of OA tibial plateaus and one of the OA synovial tissue arrays, while the down-regulated *EREG* was found down-regulated in subchondral bones of OA tibial plateaus and one of the OA synovial arrays. Additionally, *LRRC15* was up-regulated in the OA knee cartilages, synovial tissues and the subchondral bones of medial, but not lateral tibial plateau. The expression patterns of the 26 candidate genes in the OA knee cartilage dataset (GSE114007) is shown in Figure 6.

Table 3. Candidate genes of OA knee chondrocytes identified from putative targets of miRNAs.

Gene Symbol	Gene Name	HC-OA FPKM	HC FPKM	Fold-Change (HC-OA/HC)
<i>AKAP12</i>	A-kinase anchoring protein 12	94.69	32.02	2.96
<i>BASP1</i>	brain abundant, membrane attached signal protein 1	80.88	38.09	2.12
<i>BDNF</i>	brain-derived neurotrophic factor	8.28	1.76	4.70
<i>FGF7</i>	fibroblast growth factor 7	37.21	8.52	4.37
<i>GREM2</i>	gremlin 2, DAN family BMP antagonist	9.66	3.54	2.73
<i>LMOD1</i>	leiomodin 1	26.03	1.78	14.65
<i>LRRC15</i>	leucine rich repeat containing 15	6.47	2.56	2.53
<i>LRRC32</i>	leucine rich repeat containing 32	9.64	2.30	4.19
<i>MARCKS</i>	myristoylated alanine-rich protein kinase C substrate	278.54	133.99	2.08
<i>PCSK9</i>	proprotein convertase subtilisin/kexin type 9	1.51	0.53	2.86
<i>PDE3A</i>	phosphodiesterase 3A	19.30	1.88	10.25
<i>PDE7B</i>	phosphodiesterase 7B	4.98	1.53	3.27
<i>PPM1L</i>	protein phosphatase, Mg ²⁺ /Mn ²⁺ dependent 1L	4.44	0.97	4.59
<i>RALGPS2</i>	Ral GEF with PH domain and SH3 binding motif 2	48.94	18.20	2.69
<i>RGS5</i>	regulator of G-protein signaling 5	90.50	6.24	14.50
<i>RNF152</i>	ring finger protein 152	15.71	3.83	4.10
<i>RPP25</i>	ribonuclease P/MRP 25kDa subunit	4.69	2.02	2.32
<i>SESN3</i>	sestrin 3	14.57	6.95	2.10
<i>SLIT3</i>	slit guidance ligand 3	29.08	2.46	11.80
<i>SMAD3</i>	SMAD family member 3	408.29	166.01	2.46
<i>TFPI</i>	tissue factor pathway inhibitor	56.10	8.72	6.43
<i>THSD4</i>	thrombospondin type 1 domain containing 4	3.44	0.65	5.31
<i>KIAA1644</i>	KIAA1644	22.55	61.04	0.37
<i>SEMA3A</i>	semaphorin 3A	12.52	39.96	0.31
<i>EREG</i>	epiregulin	1.50	4.65	0.32
<i>SDK2</i>	sidekick cell adhesion molecule 2	2.04	15.99	0.13

HC-OA, OA knee chondrocytes; HC, normal knee chondrocytes; FPKM, fragments per kilobase of transcript per million mapped reads.

Table 4. Analysis of 26 candidate genes in osteoarthritis-related datasets in Gene Expression Omnibus database.

GEO Accession Number	GSE114007	GSE51588		GSE55235	GSE55457
Specimen	Cartilage	Subchondral bone		Synovial tissue	
	Normal/OA	Normal/OA		Normal/OA	Normal/OA
		Medial	Lateral		
Numbers	18/20	5/20	5/20	10/10	10/10
Up-Regulated mRNA *					
<i>AKAP12</i>	DOWN	n.s. †	n.s.	n.s.	n.s.
<i>BASP1</i>	UP	n.s.	DOWN	n.s.	n.s.
<i>BDNF</i>	UP	n.s.	n.s.	n.s.	n.s.
<i>FGF7</i>	UP	n.s.	n.s. †	n.s.	n.s.
<i>GREM2</i>	n.s.	n.s.	n.s.	n.s.	n.s.
<i>LMOD1</i>	n.s.	n.s.	n.s.	DOWN	n.s.
<i>LRRC15</i>	UP	UP	n.s.	UP	UP
<i>LRRC32</i>	n.s.	n.s.	n.s.	n.s.	n.s.
<i>MARCKS</i>	UP	UP	UP	UP	n.s. †
<i>PCSK9</i>	UP	UP	n.s.	–	–
<i>PDE3A</i>	UP	UP	UP	n.s.	n.s.
<i>PDE7B</i>	n.s.	n.s.	n.s.	DOWN	n.s.
<i>PPM1L</i>	n.s.	n.s.	n.s.	–	–
<i>RALGPS2</i>	n.s.	n.s.	n.s.	n.s.	n.s.
<i>RG55</i>	n.s.	n.s.	n.s.	n.s.	n.s.
<i>RNF152</i>	n.s.	n.s.	n.s.	–	–
<i>RPP25</i>	n.s.	UP	n.s.	n.s.	n.s.
<i>SESN3</i>	n.s.	n.s.	n.s.	–	–
<i>SLIT3</i>	n.s.	UP	n.s. †	n.s. †	n.s. †
<i>SMAD3</i>	DOWN	UP	UP	n.s. †	n.s. †
<i>TFPI</i>	n.s.	n.s. †	n.s.	DOWN	n.s.
<i>THSD4</i>	DOWN	UP	UP	n.s.	n.s.
Down-Regulated mRNA *					
<i>KIAA1644</i>	UP	n.s. †	n.s.	UP	n.s.
<i>SEMA3A</i>	n.s.	n.s.	n.s.	UP	n.s.
<i>EREG</i>	n.s.	DOWN	DOWN	DOWN	n.s.
<i>SDK2</i>	n.s.	UP	UP	n.s.	n.s.

The genes and their expression patterns marked in **bold** indicated those with more consistent expression patterns in OA related datasets. * For those genes with more than one probe within the array, the expression patterns were considered consistent only if there were at least two probes with significant dysregulation in the same direction. UP, significantly up-regulated in OA ($p < 0.05$); DOWN, significantly down-regulated in OA ($p < 0.05$); n.s., non-significant between normal and OA. – indicated no identical probes within the array. † indicated there were at least two probes for the gene and the expression of the gene was significant only in one of the probes.

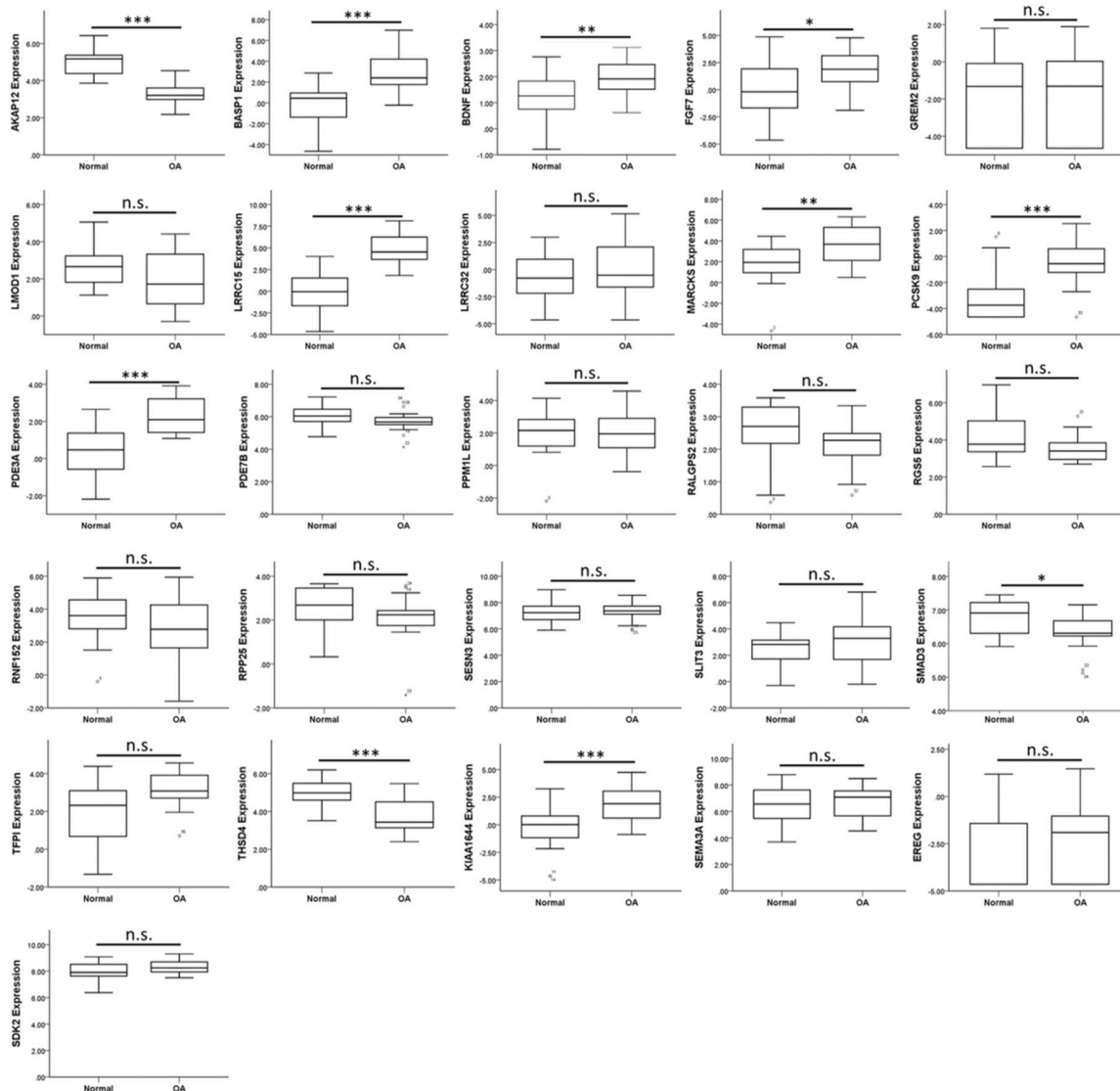


Figure 6. Analysis of 26 candidate genes with potential miRNA–mRNA interactions in the OA-related dataset. The expression values of 22 up-regulated and four down-regulated genes were analyzed in the knee cartilage dataset from GEO database (GSE114007). The significantly up-regulated expression patterns of *BASP1*, *BDNF*, *FGF7*, *LRRC15*, *MARCKS*, *PCSK9*, and *PDE3A* in OA knee cartilage were consistent with our OA chondrocytes NGS result. * indicated $p < 0.05$, ** indicated $p < 0.01$, *** indicated $p < 0.001$, and n.s. indicated no statistical significance between normal and OA groups.

3.7. Identification of Potential miRNA–mRNA Interactions of *LRRC15*, *MARCKS*, and *EREG* in OA Knee Chondrocytes

The consistent expression patterns of *LRRC15*, *MARCKS*, *PDE3A*, and *EREG* found in our NGS data and datasets of OA knee cartilages, subchondral bones and synovial tissues were analyzed in the miRmap database for potential miRNA regulations of these genes. Those potential miRNA regulations of *LRRC15*, *MARCKS*, *PDE3A*, and *EREG* with miRmap score >99.0 were selected, and matched to the 46 differentially expressed miRNAs identified from our miRNA data. The putative 3'UTR binding sites and sequences of the potential miRNA regulations identified from miRmap database were further validated in two other miRNA prediction databases, TargetScan and miRDB, and the results are listed in Table 5. There was one target binding site for miR-140-3p in the 3'UTR of *MARCKS* (Figure S3) and two target binding sites for miR-301a-3p in the 3'UTR of *EREG* (Figure S4) validated in all three miRNA prediction databases. However, no validated target binding site for miR-140-5p in the 3'UTR

of *LRRC15* was found. In addition, the target binding site for miR-495-3p in the 3'UTR of *PDE3A* was validated in miRDB, but not in the TargetScan database.

Table 5. Potential miRNA regulations of four identified genes in OA knee chondrocytes.

Down-Regulated miRNA	Fold-Change	Predicted Target Up-Regulated mRNA	miRmap Score	TargetScan	miRDB
hsa-miR-140-5p	-3.11	<i>LRRC15</i>	99.03	-	-
hsa-miR-140-3p	-2.87	<i>MARCKS</i>	99.27	+	+
hsa-miR-495-3p	-4.80	<i>PDE3A</i>	99.93	-	+
Up-Regulated miRNA	Fold-Change	Predicted Target Down-Regulated mRNA	miRmap Score	TargetScan	miRDB
hsa-miR-301a-3p	2.45	<i>REG</i>	99.06	+	+

3.8. *MARCKS* and *REG* were Potentially Involved in the Pathogenesis of Arthritic Knee Joint Pain

The 26 candidate genes were uploaded to the DAVID database and IPA software to disclose biological functions related to these differentially expressed genes of OA knee chondrocytes. The functional annotation analysis performed in the DAVID database identified 11 biological functions and their related genes; among them, three were directly related to nerve function, including axon extension, axon guidance, and synapse assembly (Table 6). The IPA network analysis of these genes yielded three categorized networks, as listed in Table 7. Network 1 related to cellular movement, cardiovascular system development and function, and organismal development possessed the highest score among the three networks, with 13 of the 26 genes involved in this network. The interconnection of molecules in network 1 is shown in Figure 7, with *MARCKS* and *REG* in the same network. The overlay diseases and functions analysis identified *BDNF*, *FGF7*, *MARCKS*, and *SEMA3A* to be associated with “outgrowth of neurite”, as indicated by the purple frame in Figure 7.

Table 6. Biological functions of 26 candidate genes in OA knee chondrocytes.

Biological Process	p-Value	Related Genes	Fold Enrichment
Negative regulation of TORC1 signaling	0.013	<i>RNF152, SESN3</i>	149.26
Cytokine-mediated signaling pathway	0.015	<i>REG, LRRC15, GREM2</i>	15.38
Axon extension involved in axon guidance	0.017	<i>SEMA3A, SLIT3</i>	111.95
cAMP catabolic process	0.021	<i>PDE7B, PDE3A</i>	89.56
Axon guidance	0.021	<i>BDNF, SEMA3A, SLIT3</i>	12.67
Oocyte maturation	0.025	<i>REG, PDE3A</i>	74.63
Positive regulation of GTPase activity	0.045	<i>RALGPS2, FGF7, REG, RGS5</i>	4.76
Negative chemotaxis	0.048	<i>SEMA3A, SLIT3</i>	39.51
MAPK cascade	0.053	<i>FGF7, REG, PPM1L</i>	7.69
Positive regulation of cell division	0.065	<i>FGF7, REG</i>	28.58
Synapse assembly	0.084	<i>BDNF, SDK2</i>	22.02

Table 7. Networks associated with 26 candidate genes differentially expressed in OA knee chondrocytes.

	Top Diseases and Functions	Score	Focus Molecules	Molecules in Network
1	Cellular Movement, Cardiovascular System Development and Function, Organismal Development	32	13	↑ AKAP12 , Akt, Ap1, ↑ BDNF , Calmodulin, Creb, ↓ EREG , ERK, ERK1/2, estrogen receptor, F Actin, ↑ FGF7 , Fibrinogen, FSH, Gsk3, Histone h3, LDL, Lh, ↑ LRRC32 , Mapk, ↑ MARCKS , ↑ PCSK9 , PDGF BB, PI3K (complex), Pka, Pkc(s), Proinsulin, Ras, ↑ RGS5 , ↓ SEMA3A , ↑ SESN3 , ↑ SLIT3 , ↑ SMAD3 , ↑ TFPI , Vegf
2	Cardiovascular Disease, Organismal Injury and Abnormalities, Cardiovascular System Development and Function	15	7	26s Proteasome, BMP2, CLU, F10, G protein alpha1, GAS6, ↑ GREM2 , HNF4A, Jnk, LPA, LRPAP1, ↑ LRRC15 , MAGI3, MAP2K5, MAP3K, MAPK9, mir-25, mir-181, MMP9, MMP12, MZB1, Neurotrophin, NFkB (complex), NRG (family), P38 MAPK, PP1/PP2A, Pp2c, ↑ PPM1L , PTPN13, ↑ RALGPS2 , ↑ RNF152 , SAA, ↓ SDK2 , ↑ THSD4 , tyrosine kinase
3	Gastrointestinal Disease, Hepatic System Disease, Organismal Injury and Abnormalities	12	6	ABCC4, AR, ↑ BASP1 , C2CD5, CENPE, CENPH, CEPT1, EGR3, ELAVL1, GADD45GIP1, INPP5K, ↓ KIAA1644 , KIF11, KIFC3, LMNB1, ↑ LMOD1 , miR-149-3p, miR-185-5p, MRRE, NONO, Pde, ↑ PDE3A , PDE4A, PDE5A, ↑ PDE7B , PFKFB3, PITX3, PLBD2, PRMT1, PSMF1, Rb, RNF14, ↑ RPP25 , TAF12, ZNF281

The genes marked in **bold** were the 26 candidate genes identified in osteoarthritic chondrocytes.

Since *MARCKS* was associated with the outgrowth of neurite, we further explored the potential roles of *MARCKS* and *EREG* on the pain condition of OA. Diseases and functions involved in the differentially expressed genes of OA knee chondrocytes were categorized using the IPA software, and networks of genes related to abnormality of cartilage tissue ($p = 5.06 \times 10^{-7}$, Z score = 1.000), proliferation of connective tissue cells ($p = 1.96 \times 10^{-9}$, Z score = 0.512), growth of neurites ($p = 6.40 \times 10^{-11}$, Z score = 0.918), and allodynia ($p = 1.68 \times 10^{-7}$, Z score = 2.547) were merged to identify the connections between *MARCKS*, *EREG* and other differentially expressed genes (Figure 8). Using the “Connect” tool in the IPA, *MARCKS* was connected to *APOE* and *CXCL12* in this merged network, while *CXCL12* was one of the molecules involved in allodynia. In addition, *EREG* was linked to *WNT5A*, *TNC*, *PTGS2*, and *TNFAIP6*.

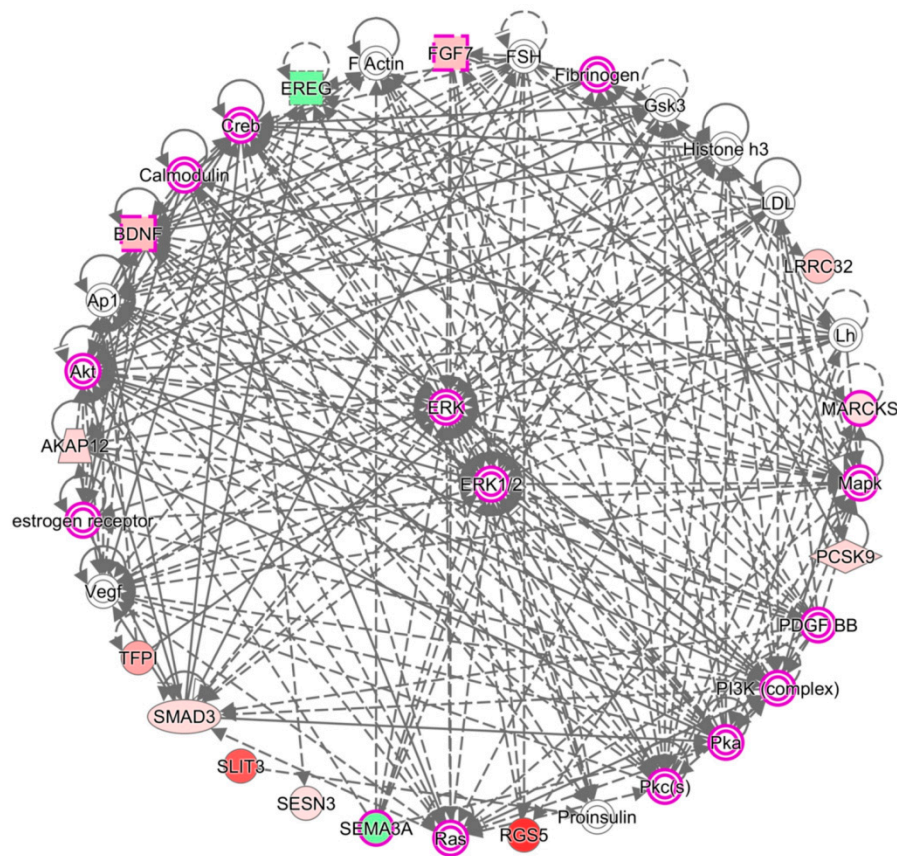


Figure 7. Network analysis by IPA identified molecules associated with the outgrowth of neurite. The network analysis of the 26 candidate genes by IPA software yielded three networks, where 13 genes were grouped into network 1, and are related to cellular movement, cardiovascular system development and function, and organismal development. The purple frames indicate molecules associated with the outgrowth of neurite, with four of our candidate genes, *BDNF*, *FGF7*, *MARCKS*, and *SEMA3A* potentially involved. Molecules with a green background indicate down-regulated expressions, and molecules with a red background indicate up-regulated expressions in OA knee chondrocytes compared to normal chondrocytes. The color scales indicate the relative expression values of OA to normal chondrocytes.

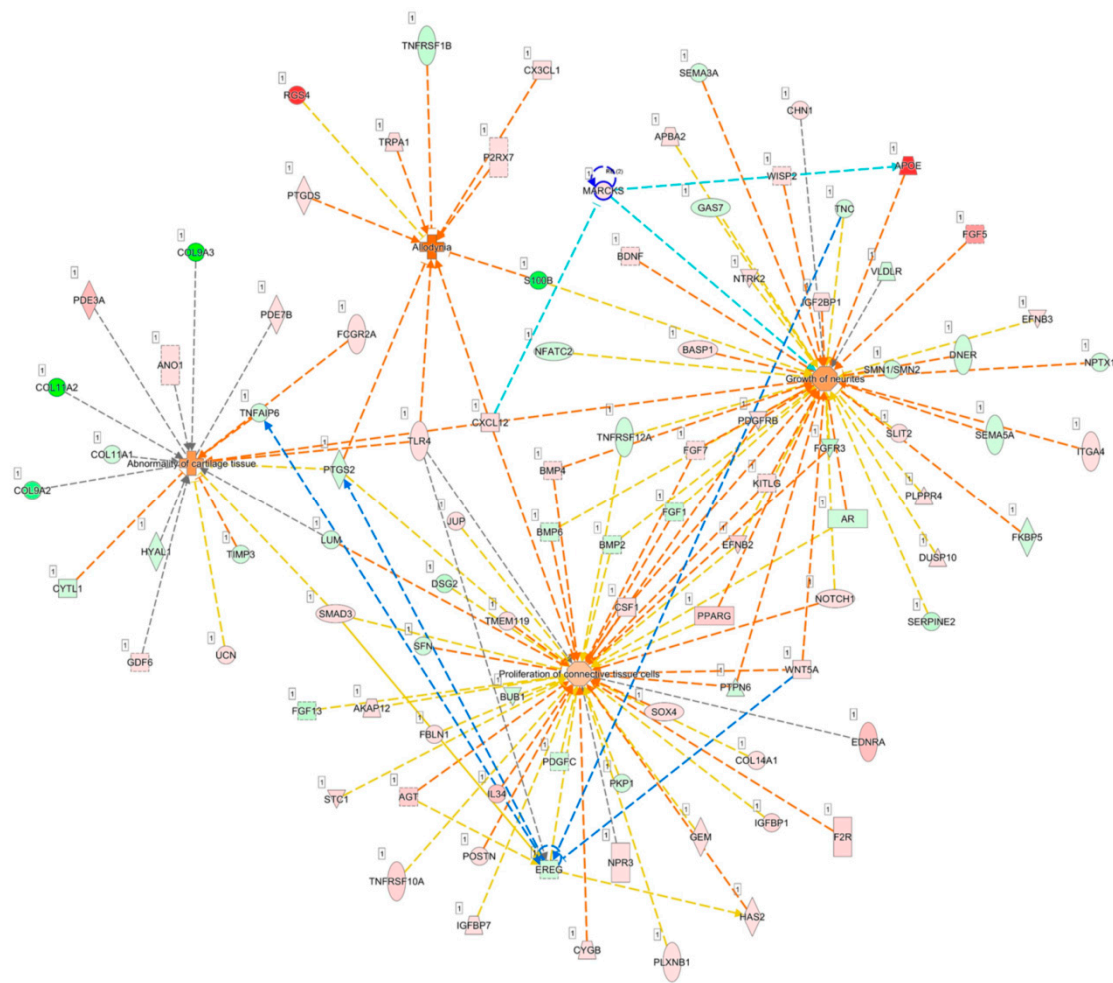


Figure 8. Analysis of the potential connections between *MARCKS*, *EREG* and OA joint pain condition. The merged network of genes related to the abnormality of cartilage tissue, proliferation of connective tissue cells, growth of neurites, and allodynia categorized from differentially expressed genes of OA knee chondrocytes by IPA software is shown. *MARCKS* was connected to *APOE* and *CXCL12*, as indicated in light blue lines, where *CXCL12* was demonstrated to be simultaneously involved in all four networks. *EREG* was mainly linked to *WNT5A*, *TNC*, *PTGS2*, and *TNFAIP6*, as indicated with blue lines.

4. Discussion

In the current study, we identified dysregulated genes related to OA joint damage from primary OA knee chondrocytes to have similar expression patterns observed in the datasets of cartilages and subchondral bones of OA knees (GSE114007 and GSE51588). Through NGS and bioinformatics analysis, we also identified 46 differentially expressed miRNAs and 26 candidate genes potentially involved in OA knee chondrocytes. Of the 26 candidate genes, *MARCKS*, *EREG*, *LRRC15*, and *PDE3A* exerted similar expression patterns as observed in the datasets of cartilages, subchondral bones and synovial tissues of OA patients. Two potential miRNA–mRNA interactions were identified, including miR-140-3p-*MARCKS* and miR-301a-3p-*EREG*, and were validated systematically. These novel miRNA regulations are proposed to play critical roles in the pathogenesis of the altered OA knee joint microenvironment and to contribute partly to arthritic joint pain.

The close anatomical contact of articular cartilage to subchondral bone, altered bone structure correlating to aggravated cartilage degeneration, increased vascularization of the bone-cartilage interface observed during OA progression, and similar presentation of epigenetic phenotypes of eroded subchondral bone and cartilage in OA suggest potential crosstalk and molecular transport

between cartilage, subchondral bone and the joint microenvironment [32–34]. The emerging role of extracellular vesicles in cartilage homeostasis and arthritis potentiated the possible mechanism of cell–cell communication between joint tissues through carriage of bioactive signaling molecules, such as miRNAs by extracellular vesicles [35–37]. Increasing evidence suggested extracellular vesicles released from chondrocytes may participate in dysregulated cartilage mineralization and contribute to OA [35,38]. Our study results identified *SMAD3* to potentially play a central role in the merged network of diseases and functions related to cellular, tissue and structural changes in OA, and serves as one of the molecules in the network of “growth of vessel” (Figure 4). In the OA joint, articular cartilage loses resistance to vascularization, and the growth of blood vessels increased particularly at the bone–cartilage interface [39]. TGF- β /SMAD2/3 signaling was shown to exert a chondroprotective effect in excessive mechanical compression by blocking chondrocyte differentiation [40]. Conversely, other studies indicated TGF- β /SMAD3 negatively regulated miR-140 in OA chondrocytes [41], and *SMAD3* was significantly up-regulated in human OA cartilage tissue [42]. Additionally, TGF- β /Smad3 treatment enhanced vascular endothelial growth factor expression and inhibited vascular smooth muscle apoptosis through autocrine signaling [43]. These results suggested that TGF- β /Smad3 may have dual roles in the vascularization of OA cartilage and the development of OA.

In a review article of WNT5A signaling, the induced WNT5A activates non-canonical Wnt signaling to regulate the control of tissue polarity and cell aggregation and canonical WNT signaling for the proliferation of human synovial fibroblasts in rheumatoid arthritis (RA) [44]. In addition, the Wnt/ β -catenin signaling is suggested to participate in the degradation of ECM in the degenerative joint of animal models by stimulating matrix catabolic genes and activity in the articular chondrocytes [45]. Recent studies also presented the positive correlation of the expression of Wnt5a in human articular cartilage to the progression of knee OA [46], and showed that Wnt5a promotes MMP production in human chondrocyte through non-canonical Wnt signaling [47]. The up-regulated WNT signaling in the inflammatory response of human chondrocytes was also proposed [48]. In the OA joint, chondrocytes aggregate to form clusters around the bone–cartilage interface [30]. Our current study identified the up-regulated *WNT5A* in OA knee chondrocytes, and bioinformatics analysis suggested the involvement of *WNT5A* in the positive regulation of cartilage development and the aggregation of cells, suggesting the important role of *WNT5A* in cartilage degradation in knee OA.

The differentially expressed miRNAs in the cartilage and bone of human knee OA with potential target genes related to inflammatory processes were identified [49]. Using the NGS and bioinformatics analysis, we identified the potential interaction of miR-140-3p-*MARCKS* in OA knee chondrocytes. Literature has identified miR-140 as a major contributor to cartilage homeostasis, targeting genes involved in the differentiation of chondrocytes [10,50]. Miyaki et al. reported the increased expression of miR-140 during chondrogenesis in human mesenchymal stem cells, the reduced expression of miR-140 in OA cartilage and in chondrocytes in response to IL-1 β , and confirmed the dual roles of miR-140 in cartilage development and homeostasis in transgenic mouse model [51,52]. In a recent study analyzing the expressions of miR-140-3p and miR-140-5p in synovial fluid of OA and non-OA patients, both miRNAs were down-regulated in OA synovial fluid and were associated with the severity of OA [53]. The down-regulated miR-140-3p and miR-140-5p were also observed in our small RNA sequencing result of OA knee chondrocytes, indicating the potential target of miR-140 as biomarkers in knee OA.

Pain is a major symptom in patients with OA. The mechanisms involved in arthritic joint pain are complicated, while structural pathologies, neuronal mechanisms of pain, and general factors such as obesity and genetic factors shall all take part in the consequence of joint pain [54]. Central and peripheral sensitizations of the nociceptive system are extensively proposed mechanisms of neuronal causes of OA joint pain [55]. Normal articular cartilage lacks vascular supply and sensory innervation [56]; structural changes of innervation in OA may be potential contributors to joint pain, with an evident increase in nerve growth and vascular penetration to the meniscus [57,58].

Suri et al. also reported the presence of nerve fibers within vascular channels of OA cartilage and subchondral bone marrow, which may contribute to pain in knee OA [33]. In our current study, we identified the increased expression of *MARCKS* in OA knee chondrocytes, and observed the similar expression patterns of *MARCKS* in OA subchondral bones and synovial tissues. Myristoylated alanine-rich protein kinase C substrate (*MARCKS*) is an actin-binding protein distributed in the nervous system and is localized in axons and dendrites; its phosphorylation is involved in the release of neurotransmitters and synaptic trafficking, mechanisms related to inflammatory pain [59]. Bradykinin is a peptide involved in inflammation, with its B2 receptors expressed on various OA-related cell types, implicating its involvement in OA pathogenesis [60]. Tanabe et al. also reported a novel bradykinin signaling cascade of neurite outgrowth through *MARCKS* phosphorylation in a neuroblastoma cell line [61]. Studies also suggested local release of neurotrophins by non-neuronal tissues in inflammatory joint lining that facilitates nerve ingrowth into tissues [62], and released neurotrophins may exert autocrine/paracrine effects that regulate articular chondrocyte metabolism [63]. This provides clues to the connection between neurite outgrowth and the pathogenesis of arthritic joint pain. There is emerging evidence regarding the possible regulatory function of miRNAs in nociceptive pathways and it is a potential therapeutic target in OA management [12]. Our current results identified the potential role of miR-140-3p-*MARCKS* regulation in the OA knee joint microenvironment. Whether targeting this novel miRNA regulation assists in the management of joint pain or not, and whether it takes part in the altered structural innervation or peripheral sensitization in knee OA merits further investigation.

Another novel miRNA regulation of miR-301a-3p-*REG* was identified in our current study. MiR-301a-3p is a pro-inflammatory miRNA that promotes inflammation during tumorigenesis [64]. There is not much literature reporting the role of miR-301a-3p in the regulation of arthritis. Two recent studies reported the regulation of miR-301a-3p in inflammatory response of RA and chondrocytes. In patients with RA, over-expressed miR-301a-3p was found in the peripheral blood mononuclear cells and it was positively correlated to an increased proportion of a subset of helper T cell [65]. Chen et al. studied the role of miR-301a in a mouse chondrogenic cell line in response to inflammatory injury using lipopolysaccharide (LPS), and reported the increased expression of miR-301a with LPS induction and the suppression of miR-301a alleviated LPS-induced chondrogenic cell injury by targeting *Sirt1*, implicating the potential therapeutic target of miR-301a for OA [66]. The down-regulated *REG* in our NGS result was the putative target of miR-301a-3p. Epregrulin (*REG*), an EGFR ligand, is expressed in various tissues; it plays important roles in wound healing and vascular remodeling during inflammation and regulates cell proliferation and differentiation [67]. A recent study by Martin et al. demonstrated the genetic association of *REG* and *EGFR* with chronic pain in patients with temporomandibular joint disorder, indicating the role of *REG* in pain processing [68]. However, the association of *REG* expression in the joint microenvironment remains unclear. Only one report demonstrated the increased expression of *REG* and pro-inflammatory cytokines in fibroblast-like synoviocytes, suggesting the role of *REG*-mediated EGFR signaling to the pathogenesis of RA [69]. In our current study, we observed the similarly down-regulated *REG* in OA knee chondrocytes, subchondral bone and synovial tissue of OA patients. Further investigation into the role of miR-301a-3p-*REG* regulation in OA may provide further insight into better understanding novel miRNA regulation in the pathogenesis of knee OA.

The characteristic change of OA is cartilage breakdown, but a growing consensus has proposed OA as a disease of the whole joint, involving all joint tissues [9]. In the current study, we identified several important molecules involved in the structural damage of OA knee joint and explored novel miRNA-mRNA regulations potentially involved in the pathogenesis of OA joint pain. The schematic potential molecular signatures and miRNA regulations related to OA structural damage and joint pain are summarized in Figure 9. These identified novel miRNA-mRNA regulations may provide new insights into the potential targets for arthritic joint pain. Further validation with experimental studies on clinical OA knee cartilage specimens are necessary to consolidate the clinical significance of the current *in silico* results.

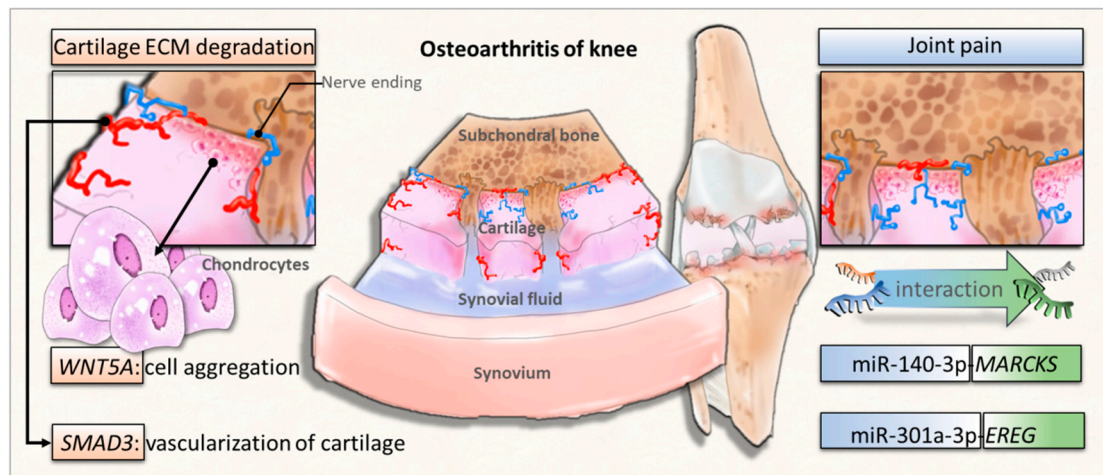


Figure 9. The proposed novel molecular signatures and miRNA regulations in osteoarthritic knee chondrocytes.

5. Conclusions

Our current study identified the critical roles of *SMAD3* and *WNT5A* in the OA knee joint microenvironment, which is potentially linked to features of ECM degradation in knee OA. Additionally, miR-140-3p-*MARCKS* and miR-301a-3p-*EREG* regulations were potentially involved in the pathogenesis of the altered OA knee joint microenvironment. The current findings suggest new perspectives in studying novel genes potentially contributing to arthritic joint pain in knee OA, which may assist in finding new targets for OA treatment.

Supplementary Materials: The following are available online at <http://www.mdpi.com/2077-0383/7/12/535/s1>, Table S1: Available information of selected osteoarthritis related datasets from GEO database, Table S2: RNA and small RNA sequencing summary, Table S3: The list of 495 differentially expressed genes in OA knee chondrocytes, Table S4: The list of 46 differentially expressed miRNAs in OA knee chondrocytes, Figure S1: RNA sequencing quality control report for normal adult chondrocytes (HC) and osteoarthritic knee chondrocytes (HC-OA), Figure S2: Small RNA sequencing quality control report for HC and HC-OA, Figure S3: The putative 3'UTR binding site of miR-140-3p on *MARCKS*, Figure S4: The putative 3'UTR binding site of miR-301a-3p on *EREG*.

Author Contributions: P.-L.K., C.-H.C., and Y.-L.H. conceived and designed the experiments; Y.-J.C., W.-A.C., and L.-Y.W. performed the experiments; Y.-J.C., W.-A.C., C.-H.C., and P.-L.K. analyzed the data; Y.-J.C. wrote the manuscript; all authors contributed to the editing and final approval of the manuscript.

Funding: Ministry of Science and Technology (MOST 107-2320-B-037-011-MY3; MOST 107-2635-B-037-001; MOST 105-2314-B-037-012), Kaohsiung Medical University Hospital (KMUHS10701; KMUHS10712; KMUH105-5M54), and Kaohsiung Medical University (KMU-DK108003).

Acknowledgments: The authors thank the Center for Research Resources and Development of Kaohsiung Medical University. We also acknowledge the statistical consultation and assistance from Hung-Pin Tu of Department of Public Health and Environmental Medicine, School of Medicine, College of Medicine, Kaohsiung Medical University.

Conflicts of Interest: The authors declare no conflict of interest.

References

1. Johnson, V.L.; Hunter, D.J. The epidemiology of osteoarthritis. *Best Pract. Res. Clin. Rheumatol.* **2014**, *28*, 5–15. [[CrossRef](#)] [[PubMed](#)]
2. MacDonald, K.V.; Sanmartin, C.; Langlois, K.; Marshall, D.A. Symptom onset, diagnosis and management of osteoarthritis. *Health Rep.* **2014**, *25*, 10–17. [[PubMed](#)]
3. Cross, M.; Smith, E.; Hoy, D.; Nolte, S.; Ackerman, I.; Fransen, M.; Bridgett, L.; Williams, S.; Guillemin, F.; Hill, C.L.; et al. The global burden of hip and knee osteoarthritis: Estimates from the global burden of disease 2010 study. *Ann. Rheum. Dis.* **2014**, *73*, 1323–1230. [[CrossRef](#)] [[PubMed](#)]

4. Findlay, D.M.; Atkins, G.J. Osteoblast-chondrocyte interactions in osteoarthritis. *Curr Osteoporos Rep.* **2014**, *12*, 127–134. [[CrossRef](#)]
5. Zhong, L.; Huang, X.; Karperien, M.; Post, J.N. The Regulatory Role of Signaling Crosstalk in Hypertrophy of MSCs and Human Articular Chondrocytes. *Int J. Mol. Sci.* **2015**, *16*, 19225–19247. [[CrossRef](#)]
6. Pesesse, L.; Sanchez, C.; Delcour, J.P.; Bellahcene, A.; Baudouin, C.; Msika, P.; Henrotin, Y. Consequences of chondrocyte hypertrophy on osteoarthritic cartilage: Potential effect on angiogenesis. *Osteoarthr. Cartil.* **2013**, *21*, 1913–1923. [[CrossRef](#)]
7. Schroepfel, J.P.; Crist, J.D.; Anderson, H.C.; Wang, J. Molecular regulation of articular chondrocyte function and its significance in osteoarthritis. *Histol. Histopathol.* **2011**, *26*, 377–394. [[CrossRef](#)]
8. Lories, R.J.; Luyten, F.P. The bone-cartilage unit in osteoarthritis. *Nat. Rev. Rheumatol.* **2011**, *7*, 43–49. [[CrossRef](#)]
9. Yuan, X.L.; Meng, H.Y.; Wang, Y.C.; Peng, J.; Guo, Q.Y.; Wang, A.Y.; Lu, S.B. Bone-cartilage interface crosstalk in osteoarthritis: Potential pathways and future therapeutic strategies. *Osteoarthr. Cartil.* **2014**, *22*, 1077–1089. [[CrossRef](#)]
10. Sondag, G.R.; Haqqi, T.M. The Role of MicroRNAs and Their Targets in Osteoarthritis. *Curr. Rheumatol. Rep.* **2016**, *18*, 56. [[CrossRef](#)]
11. Miyaki, S.; Asahara, H. Macro view of microRNA function in osteoarthritis. *Nat. Rev. Rheumatol.* **2012**, *8*, 543–552. [[CrossRef](#)] [[PubMed](#)]
12. Nugent, M. MicroRNAs: Exploring new horizons in osteoarthritis. *Osteoarthr. Cartil.* **2016**, *24*, 573–580. [[CrossRef](#)] [[PubMed](#)]
13. Zhao, M.; Liu, D.; Qu, H. Systematic review of next-generation sequencing simulators: Computational tools, features and perspectives. *Brief Funct. Genomics* **2017**, *16*, 121–128. [[CrossRef](#)] [[PubMed](#)]
14. Lewallen, E.A.; Bonin, C.A.; Li, X.; Smith, J.; Karperien, M.; Larson, A.N.; Lewallen, D.G.; Cool, S.M.; Westendorf, J.J.; Krych, A.J.; et al. The synovial microenvironment of osteoarthritic joints alters RNA-seq expression profiles of human primary articular chondrocytes. *Gene* **2016**, *591*, 456–464. [[CrossRef](#)] [[PubMed](#)]
15. Asahara, H. Current Status and Strategy of microRNA Research for Cartilage Development and Osteoarthritis Pathogenesis. *J. Bone Metab.* **2016**, *23*, 121–127. [[CrossRef](#)]
16. Huang da, W.; Sherman, B.T.; Lempicki, R.A. Bioinformatics enrichment tools: paths toward the comprehensive functional analysis of large gene lists. *Nucleic Acids Res.* **2009**, *37*, 1–13. [[CrossRef](#)] [[PubMed](#)]
17. Thomas, S.; Bonchev, D. A survey of current software for network analysis in molecular biology. *Hum. Genomics* **2010**, *4*, 353–360. [[CrossRef](#)]
18. Huang da, W.; Sherman, B.T.; Lempicki, R.A. Systematic and integrative analysis of large gene lists using DAVID bioinformatics resources. *Nat. Protoc.* **2009**, *4*, 44–57. [[CrossRef](#)] [[PubMed](#)]
19. Clough, E.; Barrett, T. The Gene Expression Omnibus Database. *Methods Mol. Biol.* **2016**, *1418*, 93–110. [[CrossRef](#)] [[PubMed](#)]
20. Vejnar, C.E.; Blum, M.; Zdobnov, E.M. miRmap web: Comprehensive microRNA target prediction online. *Nucleic Acids Res.* **2013**, *41*, W165–W168. [[CrossRef](#)] [[PubMed](#)]
21. Vejnar, C.E.; Zdobnov, E.M. MiRmap: Comprehensive prediction of microRNA target repression strength. *Nucleic Acids Res.* **2012**, *40*, 11673–11683. [[CrossRef](#)] [[PubMed](#)]
22. Stokowy, T.; Eszlinger, M.; Świerniak, M.; Fajewicz, K.; Jarzab, B.; Paschke, R.; Krohn, K. Analysis options for high-throughput sequencing in miRNA expression profiling. *BMC Res. Notes.* **2014**, *7*, 144. [[CrossRef](#)] [[PubMed](#)]
23. Hart, T.; Komori, H.K.; LaMere, S.; Podshivalova, K.; Salomon, D.R. Finding the active genes in deep RNA-seq gene expression studies. *BMC Genomics* **2013**, *14*, 778. [[CrossRef](#)] [[PubMed](#)]
24. Baras, A.S.; Mitchell, C.J.; Myers, J.R.; Gupta, S.; Weng, L.C.; Ashton, J.M.; Cornish, T.C.; Pandey, A.; Halushka, M.K. miRge—A Multiplexed Method of Processing Small RNA-Seq Data to Determine MicroRNA Entropy. *PLoS ONE* **2015**, *10*, e0143066. [[CrossRef](#)] [[PubMed](#)]
25. Krämer, A.; Green, J.; Pollard, J., Jr.; Tugendreich, S. Causal analysis approaches in Ingenuity Pathway Analysis. *Bioinformatics* **2014**, *30*, 523–530. [[CrossRef](#)]
26. Trapnell, C.; Roberts, A.; Goff, L.; Pertea, G.; Kim, D.; Kelley, D.R.; Pimentel, H.; Salzberg, S.L.; Rinn, J.L.; Pachter, L. Differential gene and transcript expression analysis of RNA-seq experiments with TopHat and Cufflinks. *Nat. Protoc.* **2012**, *7*, 562–578. [[CrossRef](#)]

27. García-Campos, M.A.; Espinal-Enríquez, J.; Hernández-Lemus, E. Pathway Analysis: State of the Art. *Front. Physiol.* **2015**, *6*, 383. [[CrossRef](#)]
28. Noble, W.S. How does multiple testing correction work? *Nat. Biotechnol.* **2009**, *27*, 1135–1137. [[CrossRef](#)]
29. Streiner, D.L. Best (but oft-forgotten) practices: The multiple problems of multiplicity—whether and how to correct for many statistical tests. *Am. J. Clin. Nutr.* **2015**, *102*, 721–728. [[CrossRef](#)]
30. Goldring, M.B.; Marcu, K.B. Epigenomic and microRNA-mediated regulation in cartilage development, homeostasis, and osteoarthritis. *Trends Mol. Med.* **2012**, *18*, 109–118. [[CrossRef](#)]
31. Bioinformatics & Evolutionary Genomics. Available online: <http://bioinformatics.psb.ugent.be/webtools/Venn/> (accessed on 27 December 2017).
32. Chen, Y.; Wang, T.; Guan, M.; Zhao, W.; Leung, F.K.; Pan, H.; Cao, X.; Guo, X.E.; Lu, W.W. Bone turnover and articular cartilage differences localized to subchondral cysts in knees with advanced osteoarthritis. *Osteoarthr. Cartil.* **2015**, *23*, 2174–2183. [[CrossRef](#)] [[PubMed](#)]
33. Suri, S.; Gill, S.E.; Massena de Camin, S.; Wilson, D.; McWilliams, D.F.; Walsh, D.A. Neurovascular invasion at the osteochondral junction and in osteophytes in osteoarthritis. *Ann. Rheum. Dis.* **2007**, *66*, 1423–1428. [[CrossRef](#)] [[PubMed](#)]
34. Jeffries, M.A.; Donica, M.; Baker, L.W.; Stevenson, M.E.; Annan, A.C.; Beth Humphrey, M.; James, J.A.; Sawalha, A.H. Genome-Wide DNA Methylation Study Identifies Significant Epigenomic Changes in Osteoarthritic Subchondral Bone and Similarity to Overlying Cartilage. *Arthritis Rheumatol.* **2016**, *68*, 1403–1414. [[CrossRef](#)] [[PubMed](#)]
35. Miyaki, S.; Lotz, M.K. Extracellular vesicles in cartilage homeostasis and osteoarthritis. *Curr. Opin. Rheumatol.* **2018**, *30*, 129–135. [[CrossRef](#)]
36. Lin, Z.; Rodriguez, N.E.; Zhao, J.; Ramey, A.N.; Hyzy, S.L.; Boyan, B.D.; Schwartz, Z. Selective enrichment of microRNAs in extracellular matrix vesicles produced by growth plate chondrocytes. *Bone* **2016**, *88*, 47–55. [[CrossRef](#)]
37. Kato, T.; Miyaki, S.; Ishitobi, H.; Nakamura, Y.; Nakasa, T.; Lotz, M.K.; Ochi, M. Exosomes from IL-1 β stimulated synovial fibroblasts induce osteoarthritic changes in articular chondrocytes. *Arthritis Res. Ther.* **2014**, *16*, R163. [[CrossRef](#)] [[PubMed](#)]
38. Rosenthal, A.K. Articular cartilage vesicles and calcium crystal deposition diseases. *Curr. Opin. Rheumatol.* **2016**, *28*, 127–132. [[CrossRef](#)] [[PubMed](#)]
39. Mapp, P.I.; Walsh, D.A. Mechanisms and targets of angiogenesis and nerve growth in osteoarthritis. *Nat. Rev. Rheumatol.* **2012**, *8*, 390–398. [[CrossRef](#)] [[PubMed](#)]
40. Madej, W.; van Caam, A.; Blaney Davidson, E.N.; van der Kraan, P.M.; Buma, P. Physiological and excessive mechanical compression of articular cartilage activates Smad2/3P signaling. *Osteoarthr. Cartil.* **2014**, *22*, 1018–1025. [[CrossRef](#)]
41. Tardif, G.; Pelletier, J.P.; Fahmi, H.; Hum, D.; Zhang, Y.; Kapoor, M.; Martel-Pelletier, J. NFAT3 and TGF- β /SMAD3 regulate the expression of miR-140 in osteoarthritis. *Arthritis Res. Ther.* **2013**, *15*, R197. [[CrossRef](#)]
42. Aref-Eshghi, E.; Liu, M.; Razavi-Lopez, S.B.; Hirasawa, K.; Harper, P.E.; Martin, G.; Furey, A.; Green, R.; Sun, G.; Rahman, P.; et al. SMAD3 Is Upregulated in Human Osteoarthritic Cartilage Independent of the Promoter DNA Methylation. *J. Rheumatol.* **2016**, *43*, 388–394. [[CrossRef](#)] [[PubMed](#)]
43. Shi, X.; Guo, L.W.; Seedial, S.M.; Si, Y.; Wang, B.; Takayama, T.; Suwanabol, P.A.; Ghosh, S.; DiRenzo, D.; Liu, B.; et al. TGF- β /Smad3 inhibit vascular smooth muscle cell apoptosis through an autocrine signaling mechanism involving VEGF-A. *Cell. Death Dis.* **2014**, *5*, e1317. [[CrossRef](#)] [[PubMed](#)]
44. Katoh, M.; Katoh, M. STAT3-induced WNT5A signaling loop in embryonic stem cells, adult normal tissues, chronic persistent inflammation, rheumatoid arthritis and cancer (Review). *Int J. Mol. Med.* **2007**, *19*, 273–278. [[CrossRef](#)] [[PubMed](#)]
45. Yuasa, T.; Otani, T.; Koike, T.; Iwamoto, M.; Enomoto-Iwamoto, M. Wnt/ β -catenin signaling stimulates matrix catabolic genes and activity in articular chondrocytes: its possible role in joint degeneration. *Lab. Invest.* **2008**, *88*, 264–274. [[CrossRef](#)]
46. Li, Y.; Xiao, W.; Sun, M.; Deng, Z.; Zeng, C.; Li, H.; Yang, T.; Li, L.; Luo, W.; Lei, G. The Expression of Osteopontin and Wnt5a in Articular Cartilage of Patients with Knee Osteoarthritis and Its Correlation with Disease Severity. *Biomed. Res. Int.* **2016**, *2016*, 9561058. [[CrossRef](#)]

47. Huang, G.; Chubinskaya, S.; Liao, W.; Loeser, R.F. Wnt5a induces catabolic signaling and matrix metalloproteinase production in human articular chondrocytes. *Osteoarthr. Cartil.* **2017**, *25*, 1505–1515. [[CrossRef](#)] [[PubMed](#)]
48. Zhong, L.; Schivo, S.; Huang, X.; Leijten, J.; Karperien, M.; Post, J.N. Nitric Oxide Mediates Crosstalk between Interleukin 1beta and WNT Signaling in Primary Human Chondrocytes by Reducing DKK1 and FRZB Expression. *Int J. Mol. Sci.* **2017**, *18*, E2491. [[CrossRef](#)]
49. Jones, S.W.; Watkins, G.; Le Good, N.; Roberts, S.; Murphy, C.L.; Brockbank, S.M.; Needham, M.R.; Read, S.J.; Newham, P. The identification of differentially expressed microRNA in osteoarthritic tissue that modulate the production of TNF-alpha and MMP13. *Osteoarthr. Cartil.* **2009**, *17*, 464–472. [[CrossRef](#)]
50. Wu, C.; Tian, B.; Qu, X.; Liu, F.; Tang, T.; Qin, A.; Zhu, Z.; Dai, K. MicroRNAs play a role in chondrogenesis and osteoarthritis (review). *Int J. Mol. Med.* **2014**, *34*, 13–23. [[CrossRef](#)]
51. Miyaki, S.; Sato, T.; Inoue, A.; Otsuki, S.; Ito, Y.; Yokoyama, S.; Kato, Y.; Takemoto, F.; Nakasa, T.; Yamashita, S.; et al. MicroRNA-140 plays dual roles in both cartilage development and homeostasis. *Genes Dev.* **2010**, *24*, 1173–1185. [[CrossRef](#)]
52. Miyaki, S.; Nakasa, T.; Otsuki, S.; Grogan, S.P.; Higashiyama, R.; Inoue, A.; Kato, Y.; Sato, T.; Lotz, M.K.; Asahara, H. MicroRNA-140 is expressed in differentiated human articular chondrocytes and modulates interleukin-1 responses. *Arthritis Rheum.* **2009**, *60*, 2723–2730. [[CrossRef](#)] [[PubMed](#)]
53. Yin, C.M.; Suen, W.C.; Lin, S.; Wu, X.M.; Li, G.; Pan, X.H. Dysregulation of both miR-140-3p and miR-140-5p in synovial fluid correlate with osteoarthritis severity. *Bone Joint Res.* **2017**, *6*, 612–618. [[CrossRef](#)] [[PubMed](#)]
54. Eitner, A.; Hofmann, G.O.; Schaible, H.G. Mechanisms of Osteoarthritic Pain. Studies in Humans and Experimental Models. *Front. Mol. Neurosci.* **2017**, *10*, 349. [[CrossRef](#)] [[PubMed](#)]
55. Schaible, H.G. Mechanisms of chronic pain in osteoarthritis. *Curr. Rheumatol. Rep.* **2012**, *14*, 549–556. [[CrossRef](#)] [[PubMed](#)]
56. Grassel, S.G. The role of peripheral nerve fibers and their neurotransmitters in cartilage and bone physiology and pathophysiology. *Arthritis Res. Ther.* **2014**, *16*, 485. [[CrossRef](#)] [[PubMed](#)]
57. Ashraf, S.; Wibberley, H.; Mapp, P.I.; Hill, R.; Wilson, D.; Walsh, D.A. Increased vascular penetration and nerve growth in the meniscus: a potential source of pain in osteoarthritis. *Ann. Rheum. Dis.* **2011**, *70*, 523–529. [[CrossRef](#)]
58. Jimenez-Andrade, J.M.; Mantyh, P.W. Sensory and sympathetic nerve fibers undergo sprouting and neuroma formation in the painful arthritic joint of geriatric mice. *Arthritis Res. Ther.* **2012**, *14*, R101. [[CrossRef](#)]
59. Tatsumi, S.; Mabuchi, T.; Katano, T.; Matsumura, S.; Abe, T.; Hidaka, H.; Suzuki, M.; Sasaki, Y.; Minami, T.; Ito, S. Involvement of Rho-kinase in inflammatory and neuropathic pain through phosphorylation of myristoylated alanine-rich C-kinase substrate (MARCKS). *Neuroscience* **2005**, *131*, 491–498. [[CrossRef](#)]
60. Tenti, S.; Pascarelli, N.A.; Cheleschi, S.; Guidelli, G.M.; Fioravanti, A. The Emerging Role of Bradykinin in the Pathogenesis of Osteoarthritis and its Possible Clinical Implications. *Curr. Rheumatol. Rev.* **2016**, *12*, 177–184. [[CrossRef](#)]
61. Tanabe, A.; Shiraishi, M.; Negishi, M.; Saito, N.; Tanabe, M.; Sasaki, Y. MARCKS dephosphorylation is involved in bradykinin-induced neurite outgrowth in neuroblastoma SH-SY5Y cells. *J. Cell. Physiol.* **2012**, *227*, 618–629. [[CrossRef](#)]
62. Gruber, H.E.; Hoelscher, G.L.; Bullock, L.; Ingram, J.A.; Norton, H.J.; Hanley, E.N., Jr. Human annulus signaling cues for nerve outgrowth: In vitro studies. *J. Orthop. Res.* **2016**, *34*, 1456–1465. [[CrossRef](#)] [[PubMed](#)]
63. Grimsholm, O.; Guo, Y.; Ny, T.; Forsgren, S. Expression patterns of neurotrophins and neurotrophin receptors in articular chondrocytes and inflammatory infiltrates in knee joint arthritis. *Cells Tissues Organs.* **2008**, *188*, 299–309. [[CrossRef](#)] [[PubMed](#)]
64. Ma, X.; Yan, F.; Deng, Q.; Li, F.; Lu, Z.; Liu, M.; Wang, L.; Conklin, D.J.; McCracken, J.; Srivastava, S.; et al. Modulation of tumorigenesis by the pro-inflammatory microRNA miR-301a in mouse models of lung cancer and colorectal cancer. *Cell. Discov.* **2015**, *1*, 15005. [[CrossRef](#)] [[PubMed](#)]
65. Tang, X.; Yin, K.; Zhu, H.; Tian, J.; Shen, D.; Yi, L.; Rui, K.; Ma, J.; Xu, H.; Wang, S. Correlation Between the Expression of MicroRNA-301a-3p and the Proportion of Th17 Cells in Patients with Rheumatoid Arthritis. *Inflammation.* **2016**, *39*, 759–767. [[CrossRef](#)] [[PubMed](#)]
66. Chen, H.; Qi, J.; Bi, Q.; Zhang, S. Suppression of miR-301a alleviates LPS-induced inflammatory injury in ATDC5 chondrogenic cells by targeting Sirt1. *Int J. Clin. Exp. Pathol.* **2017**, *10*, 8991–9000.

67. Riese II, D.J.; Cullum, R.L. Epiregulin: Roles in normal physiology and cancer. *Semin. Cell Dev. Biol.* **2014**, *28*, 49–56. [[CrossRef](#)]
68. Martin, L.J.; Smith, S.B.; Khoutorsky, A.; Magnussen, C.A.; Samoshkin, A.; Sorge, R.E.; Cho, C.; Yosefpour, N.; Sivaselvachandran, S.; Tohyama, S.; et al. Epiregulin and EGFR interactions are involved in pain processing. *J. Clin. Invest.* **2017**, *127*, 3353–3366. [[CrossRef](#)] [[PubMed](#)]
69. Lahoti, T.S.; Hughes, J.M.; Kusanadi, A.; John, K.; Zhu, B.; Murray, I.A.; Gowda, K.; Peters, J.M.; Amin, S.G.; Perdew, G.H. Aryl hydrocarbon receptor antagonism attenuates growth factor expression, proliferation, and migration in fibroblast-like synoviocytes from patients with rheumatoid arthritis. *J. Pharmacol. Exp. Ther.* **2014**, *348*, 236–245. [[CrossRef](#)] [[PubMed](#)]



© 2018 by the authors. Licensee MDPI, Basel, Switzerland. This article is an open access article distributed under the terms and conditions of the Creative Commons Attribution (CC BY) license (<http://creativecommons.org/licenses/by/4.0/>).